The Electrocardiogram as an Example of Electrostatics

RUSSELL K. HOBBIE
School of Physics and Astronomy
University of Minnesota
Minneapolis, Minnesota 55455
(Received 7 December 1972)

The relationship of the electrocardiogram (EKG) to the charge distribution in the heart provides an interesting example of electrostatics for a general physics course. The qualitative features of the EKG can be explained by a simple electrostatic model which ignores the electrical conductivity of the body. This model is developed and used to explain some EKG patterns.

INTRODUCTION

In physics courses which are taken by premedical or biology students, it is a simple matter to extend the discussion of electrostatics to provide qualitative understanding of the electrical activity of the heart. If electrical conduction within the body is ignored (see Appendix), Coulomb's law can be used to show that the electrocardiogram (EKG) measures the potential distribution of a set of dipoles within the heart. This approximation is sufficient to explain the qualitative features of both normal and abnormal electrocardiograms. The EKG is seldom discussed in general physics courses because physicists usually are not familiar with it, although laboratory experiments based on it are becoming popular.[1,2] When the EKG is presented in medical school on the other hand, the simplicity of its relation to electrostatics is not considered. This paper will develop the electrostatic model relating the EKG to the electrical activity of the heart. It will also introduce the EKG to physics teachers and show how the model can be used to explain one example of a pathological change in the EKG. The arguments will be developed in sufficient detail so that a physics student can use the paper for self-study. Calculus notation will be used, but the discussion can be adapted for a noncalculus course.

DIPOLE LAYERS

Nerve and muscle cells are very similar in their electrical behavior.[3] A dipole layer on the cell wall is an important feature of each. In a muscle cell, changes in this layer precede contraction; in a nerve cell, similar changes occur as the nerve transmits a signal. Such nerve and muscle cells are cylindrical, with diameters ranging from 2×10^{-6} m to 5×10^{-4} m. Lengths range up to 1 m. The wall of each cell is an insulating layer about 5×10^{-9} m thick. In the resting state the cell is polarized, with a charge of $\pm9\times10^{-4}$ C/m^2 distributed on each side of this layer. The potential inside the cell is about -90 mV with respect to the outside. As a nerve cell transmits a signal or a muscle cell prepares to contract, a wave of depolarization sweeps the length of the cell, causing the wall to become temporarily permeable to positive ions. These ions migrate into the cell, making the interior potential zero or somewhat positive.

The simplest model to consider for approximating the electrostatic properties of the cell is two infinite, plane, parallel double layers of charge (see Fig. 1). Each double layer consists of layers of uniform charge density $+\sigma$ and $-\sigma$ separated by a distance a. Application of Gauss' law shows that the electric field in the wall has magnitude σ/ϵ_0 and that the potential in the region between the double layers is therefore[4] $-\sigma a/\epsilon_0$. Similar relationships can be derived for spherical or cylindrical double layers.[5]

Let us now consider the dipole approximation to the potential from a double layer. Consider a dipole of moment $\mathbf{m}$, consisting of charges $\pm q$ separated by a distance a, as shown in Fig. 2(a). The field for $r\gg a$ is

$$V=(1/4\pi\epsilon_0)(\mathbf{m}\cdot\mathbf{r}/r^3)=(1/4\pi\epsilon_0)(m\cos\theta/r^2). \quad (1)$$

Consider next a dipole consisting of surface charges of density $\pm\sigma$, spread over area dS and again separated by distance a [Fig. 2(b)]. The dipole moment is

$$d\mathbf{m} = \sigma a dS = \tau dS$$

and the potential is

$$dV = (\sigma a/4\pi\epsilon_0)(dS\cos\theta/r^2)$$
$$= (\tau/4\pi\epsilon_0)(dS\cos\theta/r^2). \quad (2)$$

Recalling the definition of a solid angle, $d\Omega = dS\cos\theta/r^2$, we can write this as

$$dV = \tau d\Omega/4\pi\epsilon_0. \quad (3)$$

As long as we are a large distance from the double layer compared to its thickness, we can use this equation to calculate the potential by integration. The dipole moment need not be constant, but may vary over the surface. We must remember that there is an algebraic sign associated with $d\Omega$, which is the sign of $\mathbf{m}\cdot\mathbf{r}$.

Consider the application of this equation to the two double layers of Fig. 1. If we are at point A, $\mathbf{m}\cdot\mathbf{r}$ is negative. Since τ is uniform throughout the layer and an infinite sheet subtends a solid

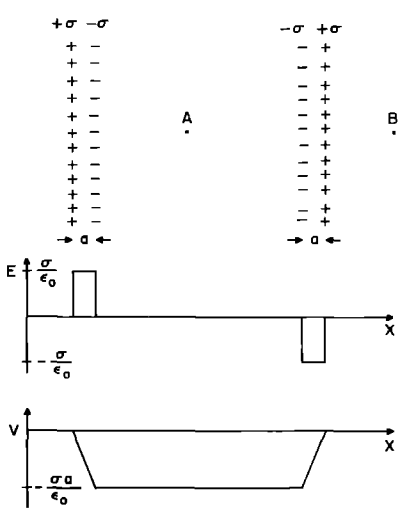

FIG. 1. Electric field and potential for two infinite, parallel, double layers, with charge $\pm\sigma$ per unit area and separation a.

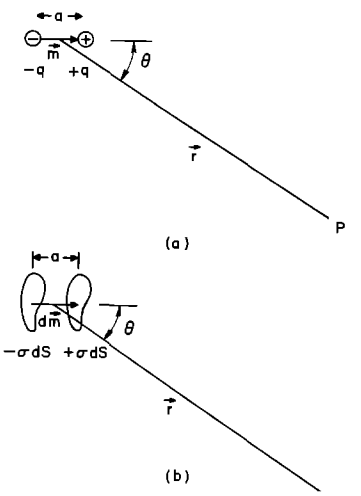

FIG. 2. Dipole of moment $\mathbf{m}$: (a) consisting of two point charges, (b) consisting of double layer of area dS.

angle 2π, the potential due to the left hand double layer is

$$V_1 = -2\pi\tau/4\pi\epsilon_0.$$

For the right hand layer $\mathbf{m}\cdot\mathbf{r}$ is also negative and one gets a like contribution. Thus the potential at point A is

$$V = -\tau/\epsilon_0 = -\sigma a/\epsilon_0, \quad (4)$$

which is in agreement with the earlier calculation. For point B, $\mathbf{m}\cdot\mathbf{r}$ is negative for the left hand double layer and positive for the right hand layer. Thus the potential at B is zero.

Whenever we have a uniform double layer of charge on a closed surface, the exterior potential will be zero. This can be seen from Fig. 3. As long as the surface is closed, for any region dS_1 which contributes to the potential there will be a corresponding region dS_2, subtending the same solid angle, for which $\mathbf{m}\cdot\mathbf{r}$ will have the opposite sign.

Consider now a nerve or muscle cell. We will neglect the fact that it is in a conducting medium and assume that it is in empty space. (The essential features of the results are unchanged by this assumption as discussed in the Appendix.[6]) In the quiescent state the cell may be regarded electrically as a long cylindrical double layer. As a signal passes along the cell, the cell wall becomes permeable to the positive charge on the

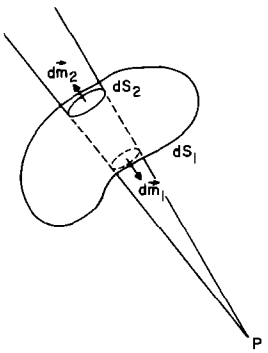

FIG. 3. The potential at an exterior point due to a uniform charged double layer on a closed surface is zero, due to cancellation of contributions for dS_1 and dS_2.

outside. These charges rush in and cause the potential difference to become zero or positive. This wave of depolarization sweeps along the cell at a velocity which is characteristic of the cell. It is about 0.3 m/sec in heart muscle, and 4 m/sec in some nerves in the heart.[7,8] Consider a cell which is depolarized for part of its length, as shown in Fig. 4(a). We wish to find the potential at some exterior point, due to the charges to the right of plane AA. The charge distribution in Fig. 4(a) is a superposition of those shown in Figs. 4(b)–(c). That in Fig. 4(b) will have no exterior potential; thus the desired potential is that due to the double layer "cap" of Fig. 4(c).

ELECTRICAL ACTIVITY OF THE HEART

The heart is an interesting example of a free-running relaxation oscillator.[9] If a heart is removed from an animal and bathed in a nutrient and oxygen supply, it will continue to beat spontaneously. Before a muscle cell contracts, a wave of depolarization sweeps over it. The contraction of the heart is initiated by spontaneous depolarization of some specialized nerve fibers located in the right atrium and called the *sino-auricular node* (SA node). The SA node acts like a free-running relaxation oscillator whose rate is accelerated by the sympathetic nerves to the heart (which release noradrenaline) and slowed by the parasympathetic nerves (which release acetylcholine).[10] Once the SA node has fired, the depolarization sweeps across both atria. There are interconnections between adjacent muscle cells, as well as a network of faster nerve fibers which allow the depolarization to spread rapidly over the entire atrium.[11] The muscles of the atria are separated from those of the ventricle by fibrous connective tissue which does not transmit the electrochemical impulse. The only connection between the atria and ventricles is some nerve tissue called the *atrio-ventricular node* (AV node). (There is some controversy as to whether the AV node is stimulated by the adjacent atrial muscle or by direct pathways from the SA node.[10]) After passing through the AV node the depolarization spreads rapidly over the ventricles on bundles of nerve cells on the inner wall of the ventricles. The parts of this network are called the common bundle (or bundle of His), the left and right bundles, and the fine network of Purkinje fibers. The AV node will undergo free running relaxation oscillations at a rate of about 50 beats/min; it usually does not free-run but is triggered by the more rapid beating of the atria. However, in well-trained athletes, the resting pulse rate may be low enough to allow the AV node to fire spontaneously, giving rise occasionally to what are known as nodal escape beats. These are physiologic and no cause for concern.

Let us now consider how the dipole moment of the heart changes with time. Initially all the heart cells are completely polarized and have no net dipole moment. The cells begin to depolarize at the SA node and this wave sweeps across the

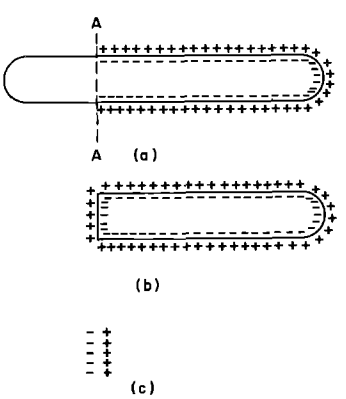

FIG 4. (a) A partially depolarized nerve or muscle cell. The charge distribution on the cell and the potential at any point may be regarded as a superposition of the closed double layer (b) and end cap (c) of opposite polarity.

atria. For each muscle cell, we can imagine a double-layer disc, perpendicular to the cell as in Fig. 4(c), with the dipole moment pointing towards the part of the cell which is still polarized. These discs for all the cells being depolarized constitute an advancing wave front.

We will now assume that we are far from the heart and neglect the fact that different dipoles

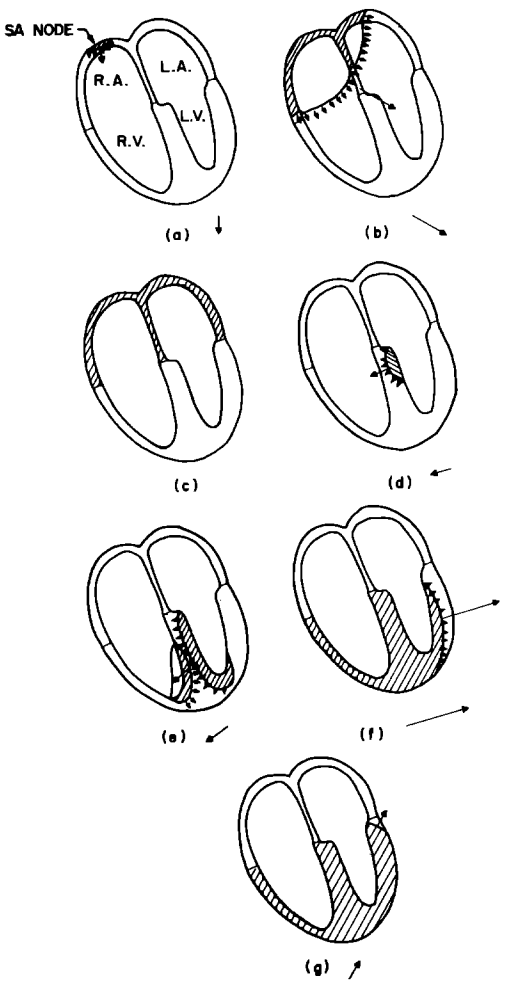

FIG. 5. Wave of depolarization sweeping over the heart. Atrial and ventricular muscle are not connected and contribute separately: (a) Depolarization beginning at SA node. (b) Atria nearly depolarized. (c) Atria completely depolarized. There is no net dipole moment. This state persists while the AV node conducts. (d) Beginning of depolarization of left ventricle. (e), (f) Continuing ventricular depolarization. (g) Ventricular depolarization nearly complete.

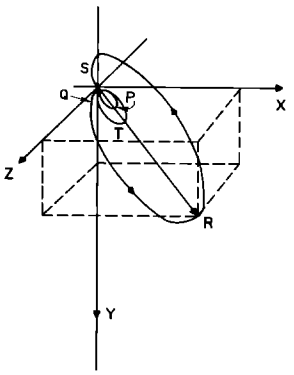

FIG. 6. Locus of the total dipole moment during the cardiac cycle.

are different distances from the point of observation. Then we may speak of the instantaneous total dipole moment as the vector sum of the dipole moments for each cell. This total dipole moment is often referred to in the medical literature as the "electric force vector" or the "activity" of the heart. Figure 5 shows how this net dipole moment changes as the myocardium depolarizes.

The wave of depolarization first travels over the atria as shown in Figs. 5(a) and (b). When the atria are completely depolarized [Fig. 5(c)] they have no net dipole moment. After passing through the AV junction, the depolarization spreads out rapidly on the inner walls of the ventricles [Fig. 5(e)–(f)] and finally travels out through the wall of each ventricle.

Repolarization of the muscle does not spread as an electrochemical wave; rather it is a diffusive process which has not been studied as well as the depolarization process.[12]

The locus of the tip of the net dipole moment **m** in a typical case is shown in the perspective drawing of Fig. 6. The x axis points to the patient's left, the y axis towards his feet, and the z axis from back to front. The small loop labelled P occurs during atrial depolarization, QRS during ventricular depolarization, and T during ventricular repolarization. Atrial repolarization is masked by the ventricular depolarization. A plot of the x, y, z components of **m** as functions of time is shown in Fig. 7. These components are typical; there can be considerable variation in the direction of the various loops of Fig. 6.

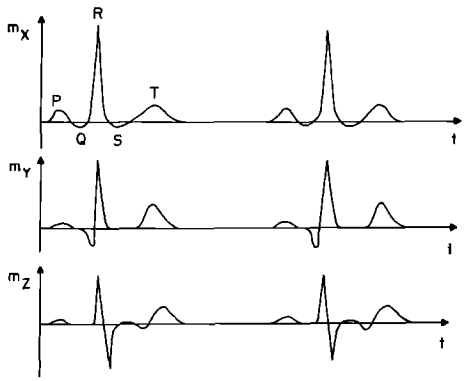

FIG. 7. The three components of the dipole moment as a function of time.

ELECTROCARDIOGRAM

Let us now consider how electrocardiographic measurements are made. We will continue to use a model in which conduction within the torso is neglected, and in which we can speak of a net dipole moment. The potential at position P due to the dipole moment $\mathbf{m}$ is then given by Eq. (1). The potential difference between two points located at $\mathbf{r}_1$ and $\mathbf{r}_2$ each a distance r from the dipole is then

$$V(\mathbf{r}_2-\mathbf{r}_1)=\mathbf{m}\cdot(\mathbf{r}_2-\mathbf{r}_1)/4\pi\epsilon_0 r^3$$
$$=\mathbf{m}\cdot\mathbf{R}/4\pi\epsilon_0 r^3.$$

Thus the potential difference between two electrodes separated by a displacement $\mathbf{R}$ and equidistant from the dipole will measure the instantaneous projection of m on R.

The standard EKG involves simultaneous measurement of twelve potential differences using 9 electrodes. This, of course, provides redundant information but does allow fairly simple interpretation. Recent work on vector electrocardiography has been directed towards finding a suitable set of leads to measure three mutually orthogonal components of $\mathbf{m}$ and to display the results in a way which can easily be interpreted.[13]

The first three electrodes are placed one on each wrist and one on the left leg. The limbs in this case serve as conductors, so the three points between which the potential differences are measured are the points where the limbs join the body. The potential differences between these points correspond to projections of $\mathbf{m}$ on $\mathbf{R}_1$, $\mathbf{R}_2$, and $\mathbf{R}_3$ (assuming the 3 points are equidistant from the heart) as shown in Fig. 8(a). These projections of $\mathbf{m}$ are labelled I, II, and III, respectively, and are called the limb leads. If the three electrodes are assumed to measure the potentials at the vertices of an equilateral triangle, then these three components have been measured along axes which are 120° apart. It is often convenient to know the components along three more axes midway between these. They are linear combinations of the first three. The reference vectors which are traditionally used are shown in Fig. 8(b). The signal which is called aV_L (augmented V_L) is the projection of $\mathbf{m}$ on a vector pointing 30° above the horizontal. (It is called aV_L because the projection is in the direction of a vector from the center of

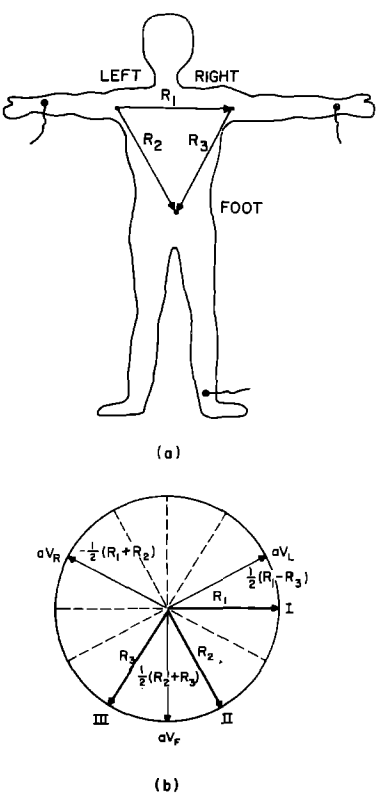

FIG. 8. (a) Position of the limb electrodes on the body, showing vectors $\mathbf{R}_1$, $\mathbf{R}_2$, and $\mathbf{R}_3$, along which the dipole moment is projected for tracings I, II and III. (b) Direction of primary projections I, II and III and derived projections aV_L, aV_R, and aV_F.

the equilateral triangle to the left shoulder.) Since I is proportional to $\mathbf{m}\cdot\mathbf{R}_1$, etc., aV_L is (I−II)/2. The other two augmented limb leads are aV_R and aV_F. Their directions are shown in Fig. 8(b). All six of these leads measure projections of **m** on a plane parallel to the chest and back, called the frontal plane.

The other six leads are placed across the chest in front of the heart and are called precordial leads. The reference potential for these leads is the sum of the potentials of the three limb electrodes, which corresponds to the potential at the center of the equilateral triangle of Fig. 8(a). Hence they measure very nearly horizontal components of **m**. They are labelled V_1–V_6, as shown in Fig. 9. Since these leads are in some cases rather close to the heart, our assumption of constant r in the integral of Eq. (3) is not satisfied. These leads are influenced most strongly by those portions of the myocardium closest to them. Waveforms for the leads of a typical normal EKG are shown in Fig. 10. The six limb leads measure components of **m** every 30° in the xy plane of Fig. 6. In particular, I is the x component and aV_F is the y component. (The graph of aV_F in Fig. 10 is not identical to m in Fig. 7 because they are for different patients.) When **m** has its greatest magnitude it is nearly parallel to II. Thus II has the largest spike, and aV_L, which is perpendicular to it, has the smallest. The projection of **m** on aV_R is negative.

The precordial leads nominally measure components in a nearly horizontal plane, although the effect of $1/r^2$ is important. The vector is strongest in the direction of V_4 and V_5. V_1 and V_6 are nearly in opposite directions and have opposite signs. In all leads the repolarization spike follows much in the same course as the depolarization, although the amplitude and duration are different.

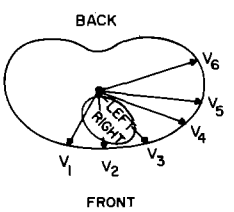

FIG. 9. Location of precordial leads and the direction of components they measure.

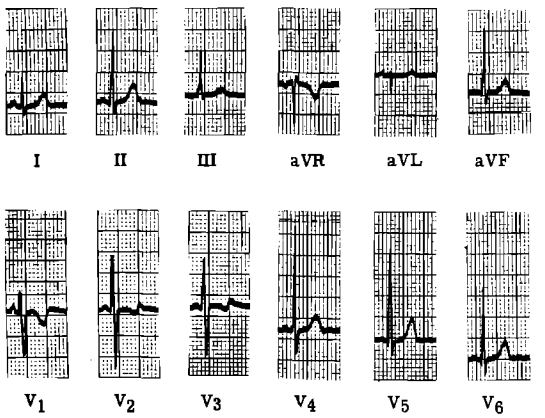

FIG. 10. Normal electrocardiogram. Large divisions are 0.5 mV vertically and 200 msec horizontally.

CHANGES IN THE ELECTROCARDIOGRAM

A detailed discussion of abnormalities in the electrocardiogram and the related pathology is beyond the scope of this paper. However, some changes can be mentioned as illustrative of the general principles involved.

The detailed shape of the QRS spike is dependent on the instantaneous vector sum of the moments in the left and right ventricles. If the right side of the heart has to pump against an abnormally heavy load for a long period of time, this exercise causes enlargement of the myocardium, a condition known as right ventricular hypertrophy. The electrocardiogram for a patient with right ventricular hypertropy is shown in Fig. 11. We see that I now has a negative spike because of the changed direction of m. In this case aV_F shows that there is very little vertical component of m. The precordial leads show the strongest signal in V_1 and V_2, because the right ventricle faces the front-right side of the body. (The extra lead V_4R is often recorded in such patients. It is symmetrical with V_4 but on the right side of the body.)

For further details on the interpretation of EKG tracings, the reader may consult many texts.[14,15] Some general principles may be mentioned. A fault in the conduction bundle, called a bundle branch block, means that the depolarization wave travels through the myocardium rather

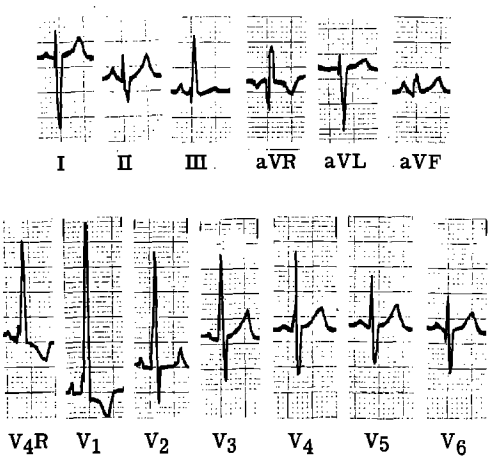

FIG. 11. Electrocardiogram of patient with right ventricular hypertrophy.

than the bundle. Since the velocity in the myocardium is low, the depolarization pulse is wider than usual. In a heart attack or myocardial infarct, a portion of the myocardium is dead and the cells neither depolarize nor repolarize. Therefore one may regard the dipole moment as being the normal one minus the dipole moment of the destroyed area. The exact nature of the changes will depend on the location of the infarct; in fact some very small infarcts are undetectable on the EKG.

SUMMARY

A simplified model of the heart suspended in a nonconducting medium has been used to relate EKG tracings to the charge distribution within the myocardium. This material is suitable for inclusion as an application of Coulomb's law in the general physics course, or as collateral reading for a laboratory experiment on the EKG. It provides a basic physical picture of the process, from which one can go on to include such effects as tissue conductivity. The model is used to correlate one example of an abnormal EKG pattern with the underlying pathological process.

ACKNOWLEDGMENTS

I wish to thank James Moller, MD, for supplying the elctrocardiograms used in Figs. 10 and 11. I am grateful to W. Albert Sullivan, MD, Assistant Dean of the University of Minnesota Medical School, for making the facilities of the Medical School available to me during the past two years.

APPENDIX

It may at first seem surprising to use an electrostatic approximation for the human body, which one usually thinks of as a conductor. An average value for its resistivity ω is 5 ohm-m.[6] However, in a medium for which the current density $\mathbf{J}$ is related to the electric field by $\mathbf{J}=\mathbf{E}/\omega$, the potential in source free regions still satisfies Laplace's equation.[16] Including sources gives

$$\nabla^2 V = \omega \nabla \cdot \mathbf{J}_i$$

where $\mathbf{J}_i$ is the source current. This problem has been discussed in detail.[6] One finds that, if the resistivity inside and outside the cell is uniform,[6]

$$V = (4\pi)^{-1} \int V_T d\Omega,$$

where V_T is the potential difference across the cell membrane ($V_{\text{outside}} - V_{\text{inside}}$). This is identical to the expression in the electrostatic case, which can be obtained by combining Eqs. (3)–(4). The charge sheets of our model are replaced by sources and sinks of current. The formalism for solving the problem in detail, considering the difference in resistivity between the cell and its membrane, is discussed in Ref. 6.

[1] H. Metcalf, Phys. Teach. **10**, 98 (1972).
[2] P. Lafrance, Phys. Teach. **10**, 462 (1972).
[3] B. Katz, *Nerve, Muscle and Synapse* (McGraw-Hill, New York, 1966).
[4] This discussion ignores the dielectric constant, κ, of the cell membrane. If it is included, the potential difference is $-\sigma a/\kappa\epsilon_0$. A typical value of κ is about 7.
[5] For the spherical double layer of radius R and thickness a, the interior potential is $V = -\sigma a R/\epsilon_0(R-a)$ while for the cylindrical case it is $V = (\sigma a/\epsilon_0)\ \ln[1-(a/R)]^{a/R}$.
[6] R. Plonsey, *Bioelectric Phenomena* (McGraw-Hill, New York, 1969), Chap. 5.
[7] *Physiology and Biophysics*, edited by T. C. Ruch and H. D. Patton (Saunders, Philadelphia, 1965), p. 576.
[8] S. Bellet, *Essentials of Cardiac Arrhythmias* (Saunders, Philadelphia, 1972), Chap. 2.
[9] A very early model of some coupled relaxation oscillators which mimicked the EKG was described by B. van der Pol and J. van der Mark, Phil. Mag. Ser. 7 **6**, 763 (1928).

A discussion of the biochemical mechanism of the relaxation oscillation is found in Ref. 8, p. 13.

[10] Katz, Ref. 3, pp. 106–107.

[11] Bellet, Ref. 8, Chap. 1.

[12] Ruch and Patton, Ref. 7, p. 582; Bellet, Ref. 8, p.12.

[13] Plonsey, Ref. 6, Chap. 6.

[14] J. R. Beckwith, *Grant's Clincial Electrocardiography: A Spatial Vector Approach* (McGraw-Hill, New York, 1970), 2nd ed.

[15] T. Winsor, *The Electrocardiogram in Myocardial Infarction* (Ciba Pharmaceutical Co., Summit, N.J., 1968).

[16] W. R. Smythe, *Static and Dynamic Electricity* (McGraw-Hill, New York, 1950), p. 231.

Continuous Quantitative Measurements on a Linear Air Track

BROTHER ERIC VOGEL, F.S.C.*
Chairman of Physics Department
Saint Mary's College of California
Moraga, California 94575
(Received 10 June 1971; revised 6 November 1972)

Described in this article is an apparatus, attachable to a linear air track, for recording the continuous motion of one or two carts over several transits of the track. The records thus produced allow one to determine the motion characteristics of the cart(s), such as velocity change during transit versus time, to an accuracy of about one percent. Also discussed are various experiments, such as acceleration due to gravity, force versus acceleration, simple harmonic motion, and collisions which have been performed using this apparatus, as well as an analysis of the basic accuracy of the data.

INTRODUCTION

The recording of the motion of carts on a linear air track has been approached by various methods, such as strobe photography[1] and forms of spark timing.[2] While strobe photography yields records that are excellent for viewing qualitative effects, the record, because of its small size, does not lend itself to detailed quantitative measurements. The apparatus described below allows the experimenter to make his measurements from a record approximately the length of the track itself, and has the important additional feature as well that many successive transits of the cart back and forth along the track can be analyzed by the experimenter.

DESCRIPTION OF THE APPARATUS

In order to achieve the continuous record mentioned above, an apparatus was designed and built to mount on an existing air track. The apparatus consists of two cylinders made of $2\frac{3}{4}$-in. diam aluminum tubing, approximately the length of the track, mounted parallel to the track by means of plastic supports on each end. The center lines of the cylinders are about level with the top of the track. Figure 1 shows a photograph of one of the plastic supports. The cylinder on the right is rigidly attached to the support, while the cylinder on the left is made rotatable by mounting a slow motor ($\frac{1}{2}$–2 rpm, Model C, Hurst, Princeton, Ind.) concentric with it. The cart, as shown in Fig. 1, has a needle mounted on a small piece of plastic to insulate it from the metal of the cart.